ELSEVIER

Virus Research 39 (1995) 129–150

Virus Research

Differentiation of filoviruses by electron microscopy [1]

T.W. Geisbert [a,*], P.B. Jahrling [b]

[a] *Pathology Division, United States Army Medical Research Institute of Infectious Diseases, Fort Detrick, Frederick, MD, 21702-5011, USA*

[b] *Virology Division, United States Army Medical Research Institute of Infectious Diseases, Fort Detrick, Frederick, MD, 21702-5011, USA*

Received 26 April 1995; revised 10 July 1995; accepted 25 July 1995

Abstract

Cultured monolayers of MA-104, Vero 76, SW-13, and DBS-FRhL-2 cells were infected with Marburg (MBG), Ebola-Sudan (EBO-S), Ebola-Zaire (EBO-Z), and Ebola-Reston (EBO-R) viruses (Filoviridae, *Filovirus*) and examined by electron microscopy to provide ultrastructural details of morphology and morphogenesis of these potential human pathogens. Replication of each filovirus was seen in all cell systems employed. Filoviral particles appeared to enter host cells by endocytosis. Filoviruses showed a similar progression of morphogenic events, from the appearance of nascent intracytoplasmic viral inclusions to formation of mature virions budded through plasma membranes, regardless of serotype or host cell. However, ultrastructural differences were demonstrated between MBG and other filoviruses. MBG virions recovered from culture fluids were uniformly shorter in mean unit length than EBO-S, EBO-Z, or EBO-R particles. Examination of filovirus-infected cells revealed that intermediate MBG inclusions were morphologically distinct from EBO-S, EBO-Z, and EBO-R inclusions. No structural difference of viral inclusion material was observed among EBO-S, EBO-Z, and EBO-R. Immunoelectron microscopy showed that the filoviral matrix protein (VP40) and nucleoprotein (NP) accumulated in EBO-Z inclusions, and were closely associated during viral morphogenesis. These details facilitate the efficient and definitive diagnosis of filoviral infections by electron microscopy.

Keywords: Ebola; Marburg; Reston; Filoviridae; Ultrastructure; Electron microscopy

[1] Disclaimer. The views of the authors do not purport to reflect the positions of the Department of the Army or the Department of Defense (para. 4-3, AR 360-5).

* Corresponding author. Tel.: +1 301-619-4803; Fax: +1 301-619-2439.

Elsevier Science B.V.
SSDI 0168-1702(95)00080-1

1. Introduction

Filovirus is the single genus of an emerging and newly characterized family of viruses recognized as Filoviridae (Kiley et al., 1982). Filoviridae, together with the Paramyxoviridae and Rhabdoviridae, comprise the order Mononegavirales (Pringle, 1991). The *Filovirus* genus is represented by two type species: Marburg virus (MBG), and Ebola virus (EBO). EBO isolates are further classified into three subtypes: Ebola-Sudan virus (EBO-S), Ebola-Zaire virus (EBO-Z), and Ebola-Reston virus (EBO-R), which can be distinguished by cross-neutralization. All except EBO-R are associated with severe, often fatal hemorrhagic fever. No antigenic cross-reactivity exists between MBG and EBO; EBO-S, EBO-Z, and EBO-R have both common and unique epitopes (Kiley et al., 1988; Sanchez et al., 1992). The nucleotide sequence differences among the three EBO subtypes is 47% with alignments containing two to three gaps, compared with a 72% divergence with six to eight gaps between EBO-Z and MBG (Feldmann et al., 1993; Sanchez et al., 1993). MBG, EBO-S, and EBO-Z are pathogenic for humans, monkeys, guinea pigs, hamsters, and mice (Murphy et al., 1990), while the recently discovered EBO-R is pathogenic for monkeys (Jahrling et al., 1990; Geisbert et al., 1992b) but apparently not humans (Centers for Disease Control, 1990). Proven prophylactic or therapeutic treatments to combat filoviral infections do not yet exist.

Previous reports of filoviral morphogenesis have been limited in part because of the necessary containment conditions associated with safe manipulation of these potential human pathogens. However, previous efforts showed that filoviruses are filamentous, pleomorphic particles varying in length up to 14,000 nm with diameters of about 80 nm. Filovirions are composed of a helical nucleocapsid (approximately 50 nm in diameter) containing a negative sense single-stranded RNA-genome (Buchmeier et al., 1983), a unit-membrane envelope derived from the host cell, and a layer of surface projections (8–10 nm in length), consisting of a single glycoprotein (GP) (Kiley et al., 1988). Kiley et al. (1982) determined that the average unit length of MBG virions purified from infected Vero cell culture supernatant was 790 nm, compared to 970 nm for EBO. While the pathway for entry of filoviruses into cells is unknown, it was proposed that filoviruses assemble in the cytoplasm of a target cell and mature by budding through the plasma membrane (Murphy et al., 1990). Specifically, accumulations of amorphous filoviral material and preformed nucleocapsids form prominent inclusion bodies, and mature virions develop when the preformed nucleocapsids acquire envelopes by passing through the host cell plasma membrane. We employed immunoelectron microscopy (IEM) to confirm that the apparent inclusion bodies were, in fact, filoviral antigen (Geisbert and Jahrling, 1990).

The current understanding of filoviral morphology and morphogenesis evolved primarily from direct observation of naturally infected humans and monkeys, experimentally infected animals, and from clinical isolations in cell culture systems (Bowen et al., 1969; Kissling et al., 1970; Murphy et al., 1971; Ellis et al., 1978a, b; Bowen et al., 1980; McCormick et al., 1983; Baskerville et al., 1985; Geisbert et al., 1992a, b). However, direct morphological comparisons among the four serotypes

using published data are not reliable because of variations in animal species, doses of inoculum, conditions of propagation, sampling periods, and methods of sample preparation. Several in vitro filoviral serotype comparisons were reported for EBO-S, EBO-Z, and MBG, but results were inconclusive (Murphy et al. 1978; Ellis et al., 1979a, b).

We previously employed IEM (Geisbert et al., 1991, 1992b) to show that EBO-R particles and intracellular inclusions reacted most intensely with EBO-R-specific polyclonal antiserum, with lesser reactivity to EBO-S and EBO-Z antisera, and with no reaction to MBG antiserum. However, cross-reactivity among EBO-R, EBO-S, and EBO-Z precluded unambiguous serotype identification. Monoclonal antibodies raised against reference filoviruses were developed, but we were unable to distinguish EBO-Z from EBO-R using these reagents in IEM assays (T.W. Geisbert, unpublished observation). Because the structural protein specificities are now known for several of these monoclonal antibodies, they can be used in IEM assays to identify morphological features associated with specific filoviral proteins.

Viral morphogenesis has been shown to depend on the host cell system employed (Matsumoto and Kawai, 1969). While the Filoviridae appear to be an ultrastructurally unique taxon, filoviruses do show some morphological similarities with other members of the order Mononegavirales. In fact, preliminary ultrastructural observations suggested classification of MBG in the Rhabdoviridae (Kissling et al., 1968). To document morphogenic features common to all filoviral infections versus features that distinguish, we investigated filoviral morphogenesis for reference strains of MBG, EBO-S, EBO-Z, and EBO-R in four different host cell systems, selected on the basis of their general utility and applicability to filoviral isolations and propagation. Ultrastructural characterization of filoviruses may assist in achieving definitive diagnosis of potential filoviral infections prior to more time consuming procedures based on cross-neutralization, and genomic sequence determinations.

2. Materials and methods

2.1. Virus, cells

The filoviral reference seeds employed included MBG (Musoke isolate), EBO-S (Boneface isolate), EBO-Z (Mayinga isolate), and EBO-R (28H isolate). MBG seed was derived from human acute phase serum collected at Nairobi Hospital (Kenya) in 1980. MBG was passaged six times through mice and six times through Vero 76 cells. EBO-S seed came from human acute phase serum obtained at Maridi Hospital during the 1976 Sudanese outbreak. EBO-S was passaged once through guinea pigs and five times through Vero 76 cells. EBO-Z seed originated from acute phase serum from a human patient collected during the 1976 Zairean outbreak. EBO-Z was passaged three times through mice and once through Vero 76 cells. EBO-R seed was derived from serum of a moribund cynomolgus monkey (*Macaca fasicularis*) obtained during the 1989 Virginia, USA epizootic. EBO-R

was passaged twice through MA-104 cells and twice through Vero 76 cells. All filoviral seeds were filtered through 0.45-μm membranes (Millipore, Bedford, MA) before use. MBG, EBO-S, EBO-Z, and EBO-R seeds, stored at −70°C, contained 6.2, 5.6, 5.3, and 6.3 $\log_{10}$ p.f.u./ml, respectively. Three continuous cell lines and one certified diploid cell strain were employed. The continuous cell lines included Vero 76, MA-104, SW-13, while DBS-FRhL-2 was the diploid strain. Vero 76 (American Type Culture Collection [ATCC], Rockville, MD) and MA-104 (Whittaker Bioproducts, Walkersville, MD) cell lines were derived from African green monkey (*Cercopithecus aethiops*) kidneys. SW-13 cells (ATCC) originated from a human adrenal cortical small-cell carcinoma. Certified DBS-FRhL-2 cells (ATCC) were generated from lung tissue of a rhesus monkey (*Macaca mulatta*). Extensive screening of DBS-FRhL-2 cells demonstrated this line free of adventitious agents and to be nontumorigenic in animals. All four cell lines were employed as stationary monolayers in Falcon 25 cm^2 sterile flasks maintained in Eagle's minimal essential medium with Earl's salts and nonessential amino acids (EMEM) and 10% heat-inactivated fetal bovine serum (FBS).

All manipulations involving infectious filoviruses were performed in a maximum containment suite (biosafety level 4) (Centers for Disease Control and National Institutes of Health, 1984) at the United States Army Medical Research Institute of Infectious Diseases (USAMRIID). Approximately 2.9 $\log_{10}$ p.f.u. of each filoviral seed was individually adsorbed in 0.5 ml volumes onto 25 cm^2 confluent monolayers of the four cell culture systems identified (e.g. MBG was inoculated onto MA-104, Vero 76, SW-13, DBS-FRhL-2, etc.). After adsorption for 1 h at 37°C, 4.5 ml of culture medium (EMEM plus 10% FBS) was added, and flasks with tightened caps were incubated at 37°C for up to 10 days. Inoculated and control flasks were serially harvested at days 2, 4, 7, and 10. Culture fluids were collected for viral infectivity titration and electron microscopy, while cells were harvested for electron microscopy. Viral infectivity was assayed on harvested fluids by counting p.f.u. on Vero 76 cells as previously described for Lassa virus (Jahrling et al., 1980).

2.2. Electron microscopy of culture fluids

Virions were recovered from culture fluids, as previously shown for EBO-R (Geisbert et al., 1991), and compared by transmission electron microscopy. Harvested fluids were fixed by 1:2 dilution in phosphate-buffered 4% paraformaldehyde plus 1% glutaraldehyde. After a 1 h fixation, 1.5 ml aliquots of the fixed-fluids were centrifuged in conical Eppendorf microcentrifuge tubes at 12,000 × g for 15 min to concentrate the virus. Supernatants were then removed, and filoviral pellets resuspended in 5–10 μl of PBS. The fixed viral suspensions were transferred to individual 200-mesh copper electron microscopy grids pre-coated with Formvar and carbon. Excess fluid was removed and grids were negatively contrasted with 1% phosphotungstic acid (pH = 6.6). Stained grids were examined with a JEOL 100 CX or 1200 EX transmission electron microscope (JEOL, Peabody, MA) at 80 kV.

2.3. Electron microscopy of cells

At days 2, 4, 7, and 10 post-inoculation (p.i.), control and inoculated cells were individually suspended in 3 ml of culture fluid, transferred to duplicate 1.5 ml conical Eppendorf microcentrifuge tubes, and loosely pelleted by centrifugation (12,000 × *g* for 30 s). Cell pellets were fixed with 2.5% glutaraldehyde in 0.1 M sodium cacodylate buffer (pH = 7.4) for 1 h and post-fixed in 1% sodium cacodylate-buffered osmium tetroxide. Cells were en-bloc stained with 0.5% uranyl acetate, dehydrated in ethanol and propylene oxide, and embedded in POLY/BED 812 resin (Polysciences, Warrington, PA). The resin was allowed to polymerize for 16 h at 60°C. Ultrathin sections were cut, placed on 200-mesh copper electron microscopy grids, stained with uranyl acetate and lead citrate, and examined with a JEOL 100 CX or 1200 EX transmission electron microscope (JEOL) at 80 kV.

2.4. Immunoelectron microscopy

Post-embedment IEM was performed on sections of MA-104 cells inoculated with MBG, EBO-S, EBO-Z, EBO-R, or control cells, harvested at day 7 p.i., as previously shown for EBO-R-infected MA-104 cells (Geisbert and Jahrling, 1990). Murine monoclonal antibodies (mouse ascitic fluids from hybridoma cells provided by the Centers for Disease Control, Atlanta, GA) employed included the following: MD04-BD07-AE11, against the VP40 protein of EBO-Z (Mayinga); DA01-AA05, against the GP protein of EBO-Z (Mayinga); HC01-AF06, against the NP protein of EBO-Z (Mayinga); and BB06-BB01, against the NP protein of MBG (Musoke). These antibodies were selected for IEM because they had defined structural protein specificities, and had been successfully employed in immunohistochemistry assays of filovirus-infected monkey tissues (B. Connolly, personal communication).

2.5. Statistical analysis of virions

One hundred virions were randomly selected for each separate treatment from day 7 p.i. cultures. Descriptive statistics were determined and mean unit lengths of filovirions were compared by using the Statview statistical analysis program (Abacus Concepts, Berkeley, CA). Descriptive statistics employed included mean unit length, standard deviation, standard error, minimum unit length, maximum unit length, variance, coefficient of variance, range, median, mode, 10% trimmed mean, plus frequency distributions. Statview employed the Bonferonni/Dunn procedure (McClave and Dietrich, 1988) at the 0.05 level of significance to compare mean unit lengths of filovirions.

3. Results

3.1. Filoviral morphogenesis

Thin-section examination of filovirus-inoculated cell cultures showed evidence of viral replication in each cell system at all sample times. Each sequential stage of

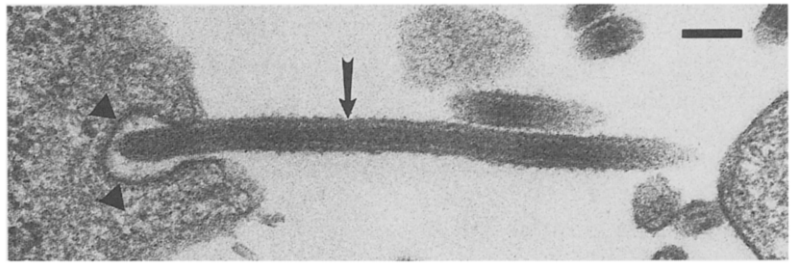

Fig. 1. Thin-section TEM shows apparent association of EBO-S virion (arrow) with coated pit (arrowheads) along plasma membrane of visibly normal MA-104 cell. Virions may enter cells by endocytosis. Bar = 120 nm.

filoviral morphogenesis was demonstrated in day 2, 4, 7, and 10 p.i. cultures, although the proportions of cells at each stage of infection may have differed. While filoviral maturation tended to progress more slowly in some cell lines than others, ultrastructural events involved in MBG, EBO-S, EBO-Z, and EBO-R morphogenesis in MA-104, Vero 76, SW-13, and DBS-FRhL-2 cells appeared to follow a similar course, regardless of cell line employed.

Filovirions appeared to be closely associated with coated pits along the plasma membrane (Fig. 1) at early sampling times, when few cells showed intracellular filoviral structures. Association of filovirions near coated pits was observed primarily in cultures sampled at day 2 p.i., and with low frequency ($\leqslant 1$ in 30 cells). The initial ultrastructural indication of filoviral infection was the presence of viral precursor material in the host cell cytoplasm. As infection progressed, viral inclusions increased in size and electron density and often occupied the entire host cell cytoplasm (morphological detail of these viral inclusions varied among serotypes and is addressed later in this report). The viral inclusions usually migrated just beneath the host cell plasma membrane where nucleocapsids, formed from viral inclusion material, acquired envelopes and associated surface projections by passing or budding through the membrane (see below).

At peak stages of viral budding, there was infrequent but intense proliferation of host cell plasma membranes (Fig. 2). By observing serial sections the possibility that this proliferation is, in fact, an increase in the number of invaginations, such as a vesicular pits or infoldings, could be excluded. Occasionally, the proliferated membranes resembled cross-sectioned filovirions while preformed nucleocapsids congregated just beneath the membraneous structures (Fig. 3). Foci of proliferated membranes seemed to be more prevalent in EBO-infected cells than in cells infected with MBG.

After preformed nucleocapsids initiated the process of budding, virions appeared to be released from the host cell by tearing away from the plasma membrane as opposed to gradual expulsion. The imperfection of this process was demonstrated by the sporadic occurrence of incomplete particles with envelopes devoid of nucleocapsids (fragments of host cell membrane) on one or both ends (Fig. 4).

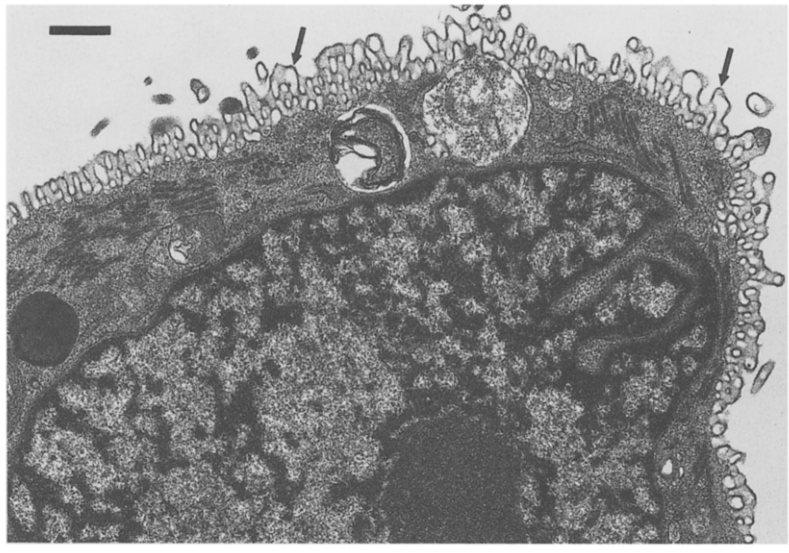

Fig. 2. Thin-section TEM illustrates proliferation of plasma membrane (Vero 76) (small arrows) infrequently observed at peak stages of filoviral production (EBO-Z). Bar = 540 nm.

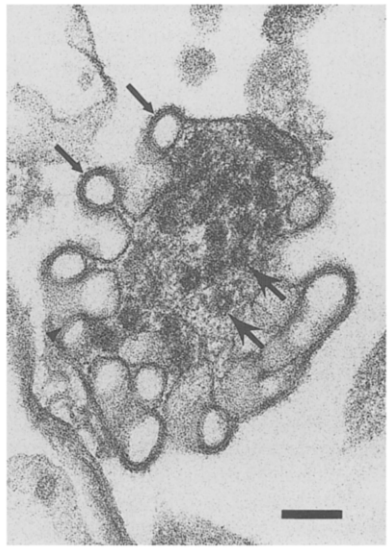

Fig. 3. Thin-section through EBO-S-infected SW-13 cell shows proliferated membranes assuming the form of filovirions (small arrows) while preformed nucleocapsids (spearheads) congregated just beneath the membraneous structures. Bar = 140 nm.

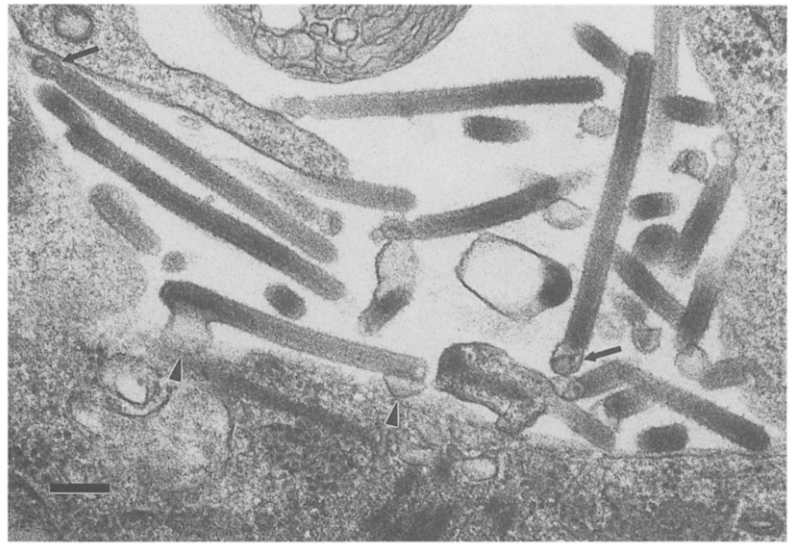

Fig. 4. Thin-section TEM shows detail of incomplete EBO-R particles. Several virions show nucleocapsid-deficient ends (small arrows), while budding particle will presumably show fragments of membrane (DBS-FRhL-2) on both poles (arrowheads) when released. Bar = 180 nm.

Some filovirus-infected cells, with viral inclusion material and budding virions, showed no ultrastructural damage of cellular organelles or cytoplasmic matrix, while others showed degenerative changes including swollen mitochondria with degenerate cristae, dilated endoplasmic reticulum, and intracytoplasmic vesiculation. Thus, it appeared that disruption of cellular organelles occurred after inclusion body formation and budding of filovirions. Infected cells responded to organelle degeneration by increased autophagosomal activity. As breakdown of cellular organelles and related lysosomal activity progressed, budding of filovirions gradually declined, nuclei became condensed, and electron density of the cytoplasmic matrix waned. Ultimately, dissolution of both plasma and nuclear membranes reduced infected cells to debris.

Although the sequence of morphogenic events was similar in all tested filovirus and cell culture systems, some morphological details differed. The most prominent morphological variation involved formation of viral inclusion material and nucleo-

Fig. 5. Thin-section TEM's demonstrating sequential events in the assembly and budding of MBG in MA-104 cells. (A) Nascent viral precursor material (arrowheads) initially appeared in cytoplasm adjacent to nucleus. Bar = 710 nm. (B) Increase in electron density of amorphous viral material plus appearance of 45–60 nm spheres (arrowheads) surrounding inclusion. Bar = 450 nm. (C) Intermediate inclusion shows dispersion of inclusion material and concomitant loss of spheres. Bar = 580 nm. (D) Final stage of MBG viral inclusion evolution. Nucleocapsids (arrowheads) appear to be formed by condensation of cylindrical inclusion material. These preformed nucleocapsids then passed through the plasma membrane to form mature virions (small arrows). Bar = 490 nm.

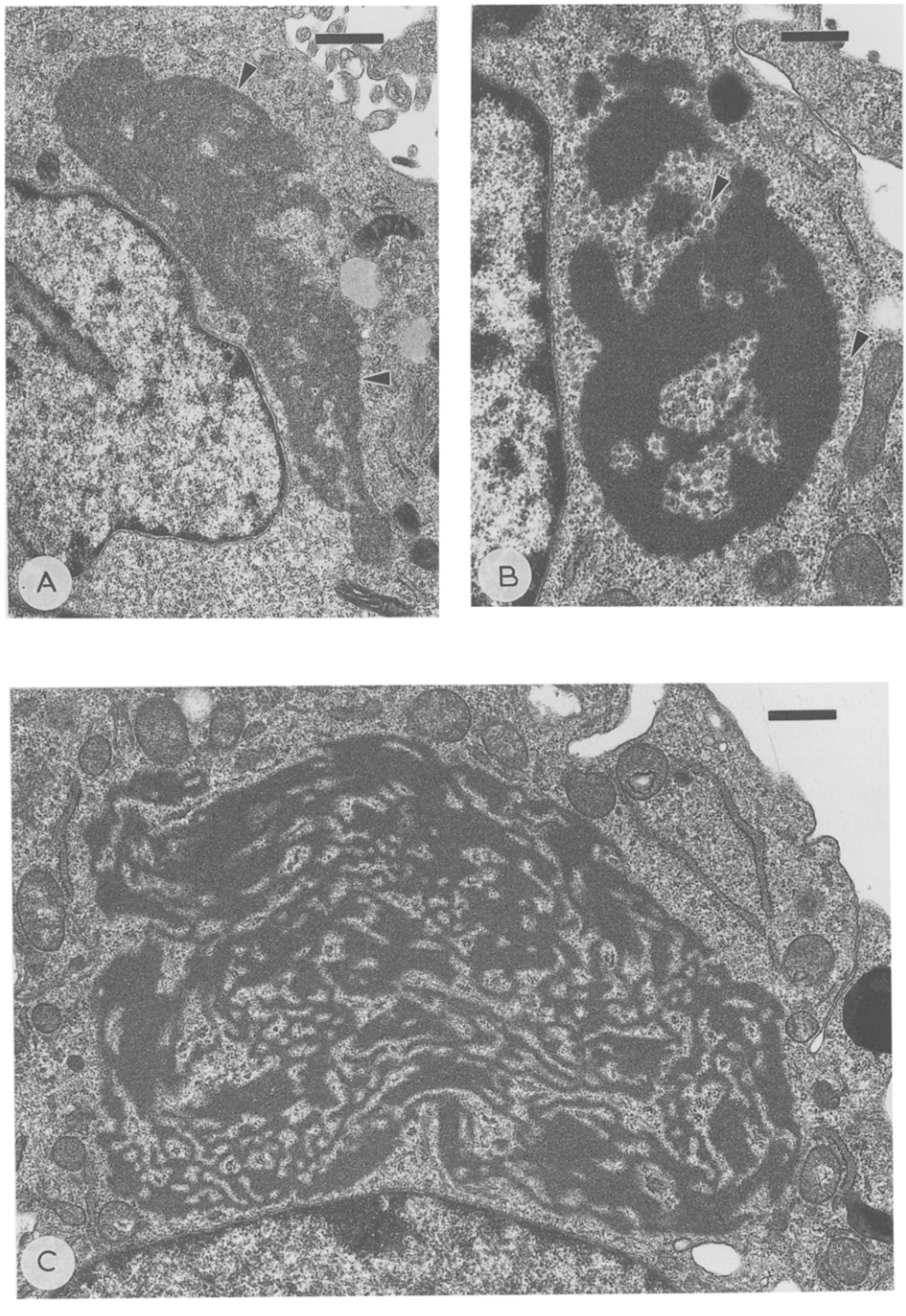
A
B
C

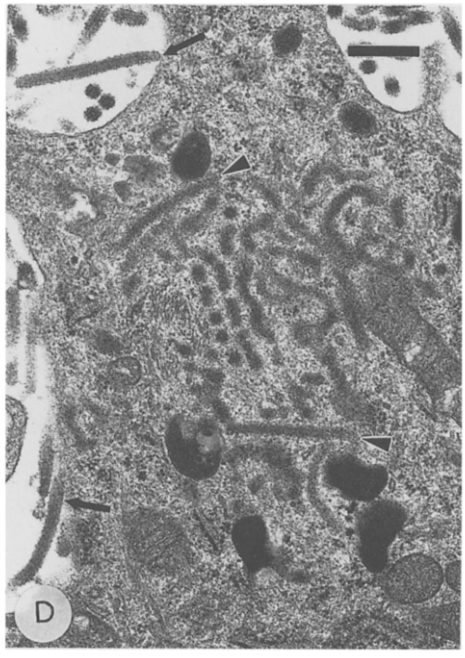

Fig. 5 (continued).

capsids of MBG. Early MBG inclusions were similar architecturally to the paler staining viral inclusions of EBO-S, EBO-Z, and EBO-R. However, MBG intermediate inclusions were easily distinguished from the other filoviruses in all cell culture systems employed. These ultrastructural differences are illustrated in Figs. 5 and 6 (most striking when comparing Fig. 5C vs. Fig. 6C). Fig. 5 shows sequential events in the assembly and budding of MBG in MA-104 cells while Fig. 6 shows the same sequence of events in MA-104 cells infected with EBO-R (the intermediate inclusions of EBO-R, EBO-S, and EBO-Z were indistinguishable in the four cell systems employed).

Intracytoplasmic MBG inclusions were usually seen as amorphous electron dense matrices or sheets surrounded by 45–60-nm spheres. MBG inclusions infrequently appeared to be comprised of tubules 20–25 nm in diameter (Fig. 7). As MBG inclusions matured, the dense matrices accumulated beneath the plasma

Fig. 6. Thin-section TEM's showing sequential events in the assembly and budding of EBO-R in MA-104 cells. (A) Nascent viral precursor material (arrowheads) initially appeared in cytoplasm adjacent to nucleus. Bar = 800 nm. (B) Increase in electron density of inclusion material plus appearance of preformed nucleocapsids (arrowheads) in early intermediate inclusion. Bar = 1.5 μm. (C) Intermediate inclusion shows dispersion of viral inclusion material and an increase in number of preformed nuclecapsids. Bar = 770 nm. (D) Final stage of EBO-R inclusion evolution. Preformed nuclecapsids (arrowheads) migrated to plasma membrane for envelope acquisition. Note preformed nucleocapsid (spearhead) in process of budding through membrane. Bar = 430 nm.

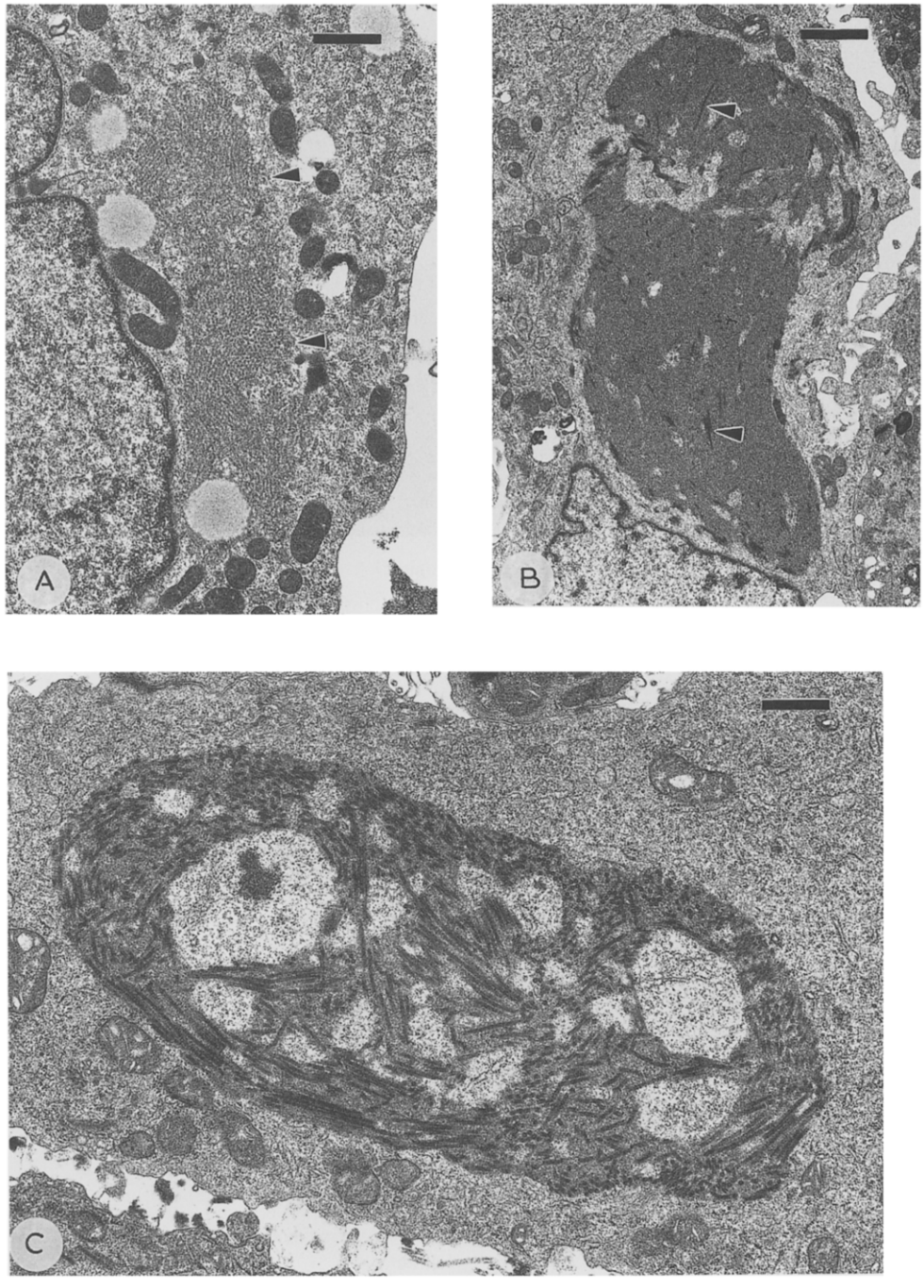
A
B
C

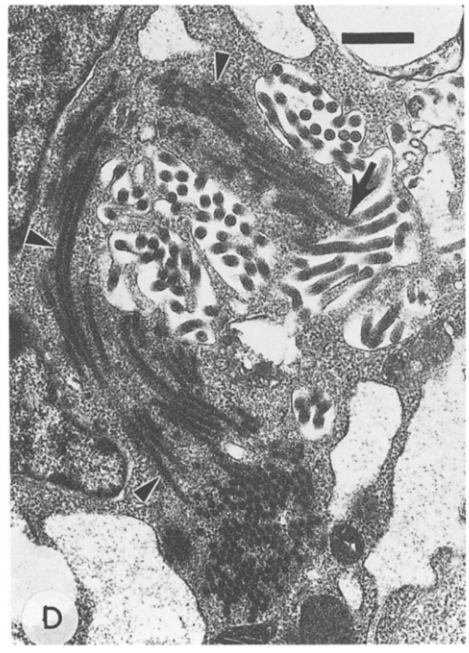

Fig. 6 (continued).

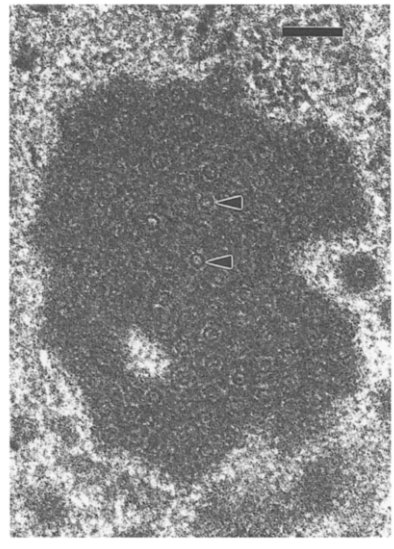

Fig. 7. Thin-section TEM shows MBG inclusions (Vero 76) infrequently appear to be comprised of tubules (arrowheads) 20–25 nm in diameter. Bar = 110 nm.

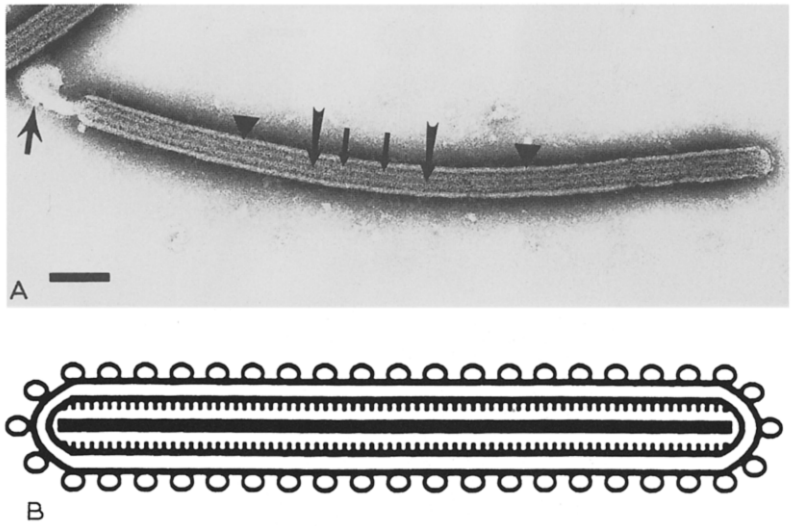

Fig. 8. Ultrastructure of a filoviral particle. A. EBO-R virion (Vero 76) by negative-contrast TEM. The virion consisted of a core (arrows) surrounded by a helical capsid (small arrows). A viral envelope (arrowheads) encircled the capsid. Empty coats (spearhead) were occasionally seen at virion poles. Bar = 170 nm. B. Schematic drawing of a filoviral particle (reproduced from International Committee on Taxonomy of Viruses, 1995, with permission of Springer-Verlag, Inc.). The nucleocapsid (about 50 nm in diameter) has a central axis or core (about 20 nm in diameter) surrounded by a helical capsid with cross-striations exhibiting a periodicity of about 5 nm.

membrane. The inclusion material then condensed into cylindrical structures which eventually assembled as nucleocapsids that budded through the plasma membrane.

In contrast, EBO-S, EBO-Z, and EBO-R inclusions were seen as amorphous matrices containing preformed nucleocapsids that were easily recognized against the less electron-dense matrix. Longitudinal sections showed preformed nucleocapsids were 900–1000 nm in length, while cross-sections demonstrated that these structures were 45–50 nm in diameter. As EBO-S, EBO-Z, and EBO-R inclusions matured, the preformed nuclecapsids increased in number and the inclusions progressed to the host cell plasma membrane. The preformed nucleocapsids then migrated from the inclusion through the membrane to secure envelopes.

3.2. Filoviral morphology

Negatively contrasted filoviral particles, regardless of serotype or host cell, contained an electron-dense 19–25-nm central axis (core) surrounded by a pale-staining helical capsid. The nucleocapsid diameter was 45–50 nm with a cross-striation interval of about 5 nm. The nucleocapsid was bound by a closely apposed unit-membrane envelope presumably derived from host cell plasma membrane. Completely developed filoviral particles were uniformly 78–80 nm in diameter

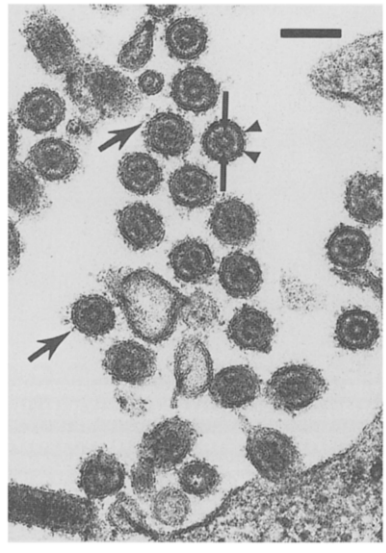

Fig. 9. As demonstrated in cross-section, each filovirion (EBO-R) contained a 45–50 nm nucleocapsid (defined by small arrows) bound by a closely apposed unit-membrane envelope (small arrowheads) derived from host cell membrane (Vero 76). Surface spikes (spearheads) were occasionally seen protruding from viral envelopes. Bar = 110 nm.

(Fig. 8). Empty envelopes or host cell membrane fragments were occasionally seen on one or both virion poles (Fig. 8A).

The viral envelope was coated with surface projections or 'spikes' 5–10 nm in length. Thin-section examination of infected cells more effectively demonstrated surface spikes (Fig. 9) than examination of negatively contrasted virions because negative staining frequently stripped off the layer of spikes. Thin-sectioned MBG spikes appeared to be more numerous and obtrusive, but often of poorer structural preservation than sectioned EBO-S, EBO-Z, or EBO-R spikes. EBO and MBG spikes were inserted into envelopes as shown by Schnittler et al. (1993) for MBG.

Negatively contrasted filovirions were pleomorphic, showing various proportions of long filaments, '6'-shaped forms, and circular configurations. Pleomorphism sorted by type species, but not cell culture systems (Table 1). MBG showed a much higher incidence of circular forms than EBO serotypes (Fig. 10). In contrast, EBO-S, EBO-Z, and EBO-R were characterized by many long filamentous virions, some '6'-shaped forms, and very few circular forms (Fig. 11). MBG appeared to show fewer disrupted or 'moth-eaten' (Ellis et al., 1979a) virions than other filoviruses, but differences were inconsistent. The sporadic occurrence of aberrant virions previously shown in tissues and cultured cells infected with EBO-S (Ellis et al., 1978a, b) was confirmed, but aberrant EBO-Z, EBO-R, and MBG virions were also seen. While EBO serotypes appeared to show higher incidences of aberrant viral particles than MBG, results were equivocal.

Table 1
Configurations of negatively contrasted Marburg, Ebola-Sudan, Ebola-Zaire, and Ebola-Reston virions recovered from four independent cell culture systems

Filovirus	Config.	MA104	Vero76	SW13	FRhL2
Marburg	Circular	33 [a]	36	38	29
	'6'-shape	58	56	56	60
	Filament	9	8	6	11
Ebola-Sudan	Circular	3	1	4	4
	'6'-shape	40	37	42	39
	Filament	57	62	54	57
Ebola-Zaire	Circular	4	2	4	2
	'6'-shape	39	36	44	43
	Filament	57	62	52	55
Ebola-Reston	Circular	0	3	5	1
	'6'-shape	36	36	38	38
	Filament	64	61	57	61

[a] Percentage of total virions of each configuration, determined from random sampling of 100 virions of each serotype and cell system.

Although nucleocapsid and particle diameters were consistent within and among serotypes, unit lengths of virions varied considerably. Evaluation of frequency distributions (data not shown) demonstrated that most filoviral particle lengths

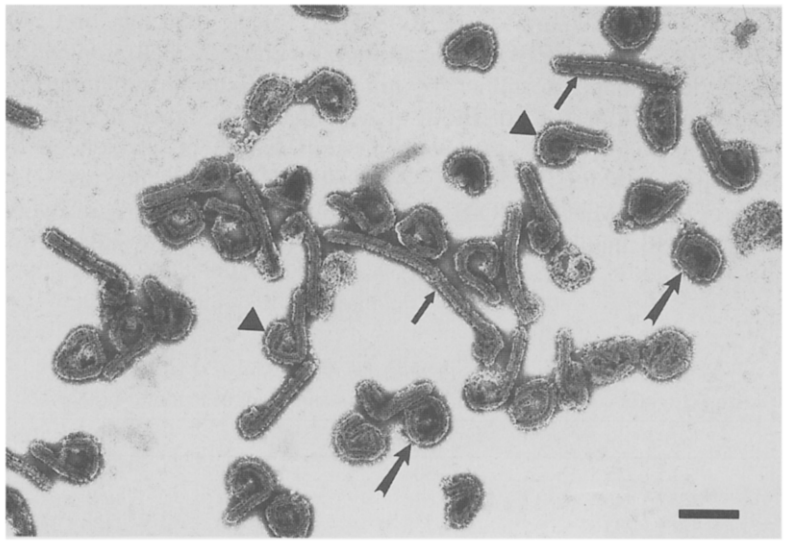

Fig. 10. Negatively contrasted MBG virions recovered from fluid of infected MA-104 cells. Note high proportion of circular (arrows) and '6'-shaped forms (arrowheads) compared to filamentous virions (small arrows). Bar = 360 nm.

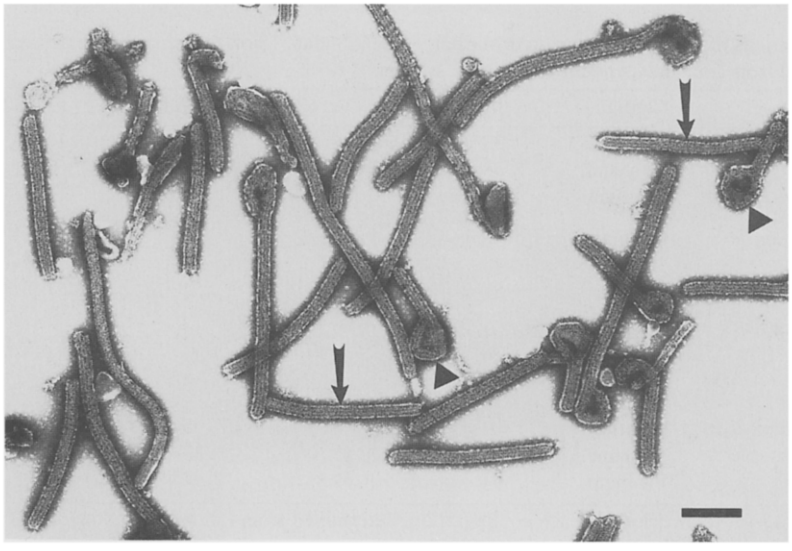

Fig. 11. Negatively contrasted EBO-R virions recovered from fluid of infected MA-104 cells. Note high proportion of filamentous forms (arrows) compared to true '6'-shaped forms (arrowheads) and no circular forms. Bar = 360 nm.

were congregated in close proximity to median unit length values, while secondary and tertiary peaks frequently occurred at values double or triple the value of that median unit length. The median unit lengths of virions ranged from 795 to 828 nm for MBG, from 974 to 1063 nm for EBO-S, from 990 to 1086 nm for EBO-Z, and from 1026 to 1083 nm for EBO-R, depending on the host cell employed. Means and standard deviations determined by randomly measuring unit lengths of each filovirus, harvested from each of the four cell lines, are shown in Table 2. MBG virions appeared to be more consistent in unit length, as evidenced by lower standard deviations, than EBO-S, EBO-Z, or EBO-R. Significance tests comparing mean unit lengths of MBG, EBO-S, EBO-Z, and EBO-R virions recovered from each cell system, distinguished MBG from EBO-S, EBO-Z, and EBO-R in all cell

Table 2
Mean unit lengths and standard deviations of Marburg, Ebola-Sudan (Ebo-S), Ebola-Zaire (Ebo-Z), and Ebola-Reston (Ebo-R) virions recovered from four independent cell culture systems

Filovirus	MA-104	Vero 76	SW-13	DBSFRhL2
Marburg	865 ± 215 [a]	890 ± 304	863 ± 245	858 ± 255
Ebo-S	1257 ± 446	1228 ± 612	1168 ± 494	1295 ± 618
Ebo-Z	1269 ± 793	1268 ± 752	1136 ± 400	1186 ± 398
Ebo-R	1255 ± 578	1168 ± 457	1133 ± 339	1170 ± 379

[a] Mean unit length (nm) and standard deviation (nm) determined from random sampling and measurement of 100 virions of each serotype and cell system.

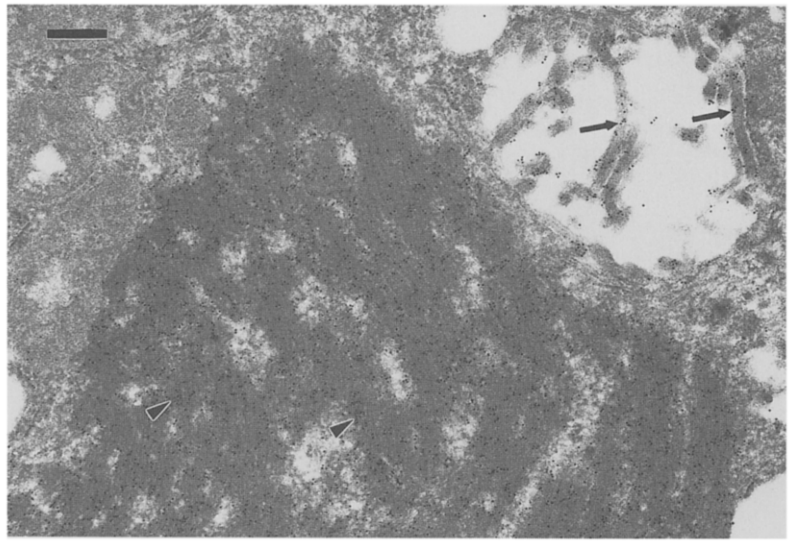

Fig. 12. Thin-section through EBO-Z-infected cell (MA-104) shows positive gold-sphere labeling of intermediate inclusion (arrowheads) and virions (small arrows) when incubated with a murine monoclonal antibody raised against a homologous viral nucleoprotein (NP). Bar = 250 nm.

lines employed. However, significance tests (at $p < 0.05$) were unable to show differences among unit lengths of EBO-S, EBO-Z, and EBO-R. While MBG was significantly shorter than the three EBO subtypes, filoviral lengths varied independently of the four cell systems tested.

3.3. Immunoelectron microscopy

EBO-Z inclusion material and particles were identified as containing homologous NP and VP40 proteins by immunogold labeling of thin-sections with the anti-NP, as shown in Fig. 12, and anti-VP40 (not illustrated) monoclonal antibodies. The EBO-Z anti-GP monoclonal did not bind to the EBO-Z inclusion material, but did label EBO-Z virions and occasionally labeled foci of proliferated membrane. EBO-S and EBO-R inclusion material and virions labeled with the EBO-Z anti-VP40 and anti-NP monoclonals, and sparsely with the EBO-Z anti-GP monoclonal. None of the EBO-Z antibodies employed labeled the plasma membrane or the nucleus of infected cells, sections of MBG-infected cells, or control sections. The MBG anti-NP monoclonal labeled MBG inclusion material (Fig. 13) and virions, but did not label EBO-S, EBO-Z, EBO-R, or control sections, or membranes and nuclear components of MBG-infected cells.

3.4. Viral infectivity titration

Differences in the replication ability of specific filoviruses when inoculated into identical hosts at equal doses were not apparent. No single serotype consistently

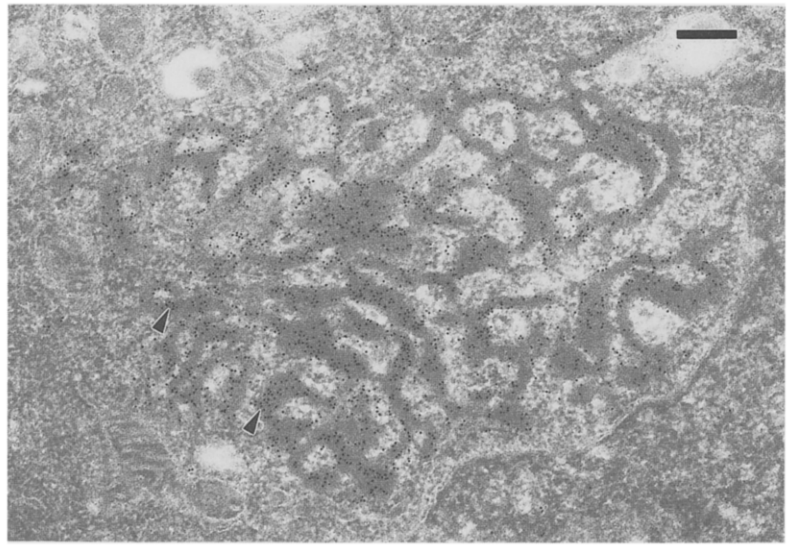

Fig. 13. Thin-section through intermediate MBG inclusion (SW-13) shows positive gold-sphere labeling (arrowheads) when incubated with a murine monoclonal antibody raised against a homologous viral nucleoprotein (NP). Bar = 250 nm.

produced more or less infectious virus than others and none of the four cell types appeared significantly more susceptible (data not shown).

4. Discussion

Transmission electron microscopy was a useful tool in diagnosis and studies of the original filoviral outbreak in 1967 (Siegert et al., 1967) and continues to facilitate the understanding and identification of filoviruses as evidenced in the 1989 simian epizootic of EBO-R (Geisbert and Jahrling, 1990). Filoviral particles and intracellular inclusions are morphologically identifiable features that can assist in the initial diagnosis of potential filoviral infections. While the filoviruses employed in this study showed a similar progression of morphogenic events, serotype-specific morphological differences were also demonstrable. In fact, MBG was morphologically distinguishable from other filoviruses without immunological assistance on the basis of its inclusions and size. EBO-S, EBO-Z, and EBO-R intermediate inclusions contained preformed nucleocapsids whereas MBG intermediate inclusions were usually seen as amorphous matrices or sheets surrounded by 45–60 nm spheres. In addition, MBG virions were significantly shorter in mean unit length than EBO-S, EBO-Z, or EBO-R virions regardless of cell culture system employed. Recent studies inoculating Vero cells with a separate MBG isolate (Ravn) showed morphological detail of intermediate MBG inclusions identical to those presented for the MBG (Musoke) isolate employed in this study

(T.W. Geisbert, unpublished observation). Murphy et al. (1978) illustrated a MBG inclusion in a Vero cell infected with a third MBG isolate that also shows morphological detail consistent with our findings. Thus, features of the intermediate viral inclusions characteristic of MBG infections can be generalized. Ultrastructural differences in surface spikes were suggested between MBG virions and other filoviruses. MBG surface spikes appeared to be more disrupted by processing procedures we employed than EBO spikes. This structural disparity may be related to the composition of the GP proteins. EBO-Z, EBO-S, and EBO-R isolates contained abundant amounts of terminal sialic acids on N- and O-linked glycans, while MBG isolates were devoid of terminal sialic acid (Geyer et al., 1992).

While aberrant virions previously associated with EBO-S-infected cells (Ellis et al., 1978a, b) were seen, we also observed aberrant EBO-Z, EBO-R, and MBG virions. Thus, definitive serotype identification founded on this structural feature was not possible. Overall, observation of intermediate viral inclusions should be the most definitive and efficient morphologic method of identifying filoviral serotypes since repeated measures and statistical comparisons of virion sizes are unnecessary, and because inclusions are striking features that are more easily evaluated than spikes. Therefore, structural differentiation of filoviruses, at least MBG from EBO-S, EBO-Z, and EBO-R, by visualization of intermediate inclusions, may augment immunologically based diagnostic assays and provide early definitive viral identification.

Our observations confirmed some structural similarities between filoviruses and other members of Mononegavirales, but filoviral particles were clearly distinguishable by electron microscopy. We were able to demonstrate morphogenic similarities among filoviruses and members of Paramyxoviridae. Nascent filoviral inclusions (best shown by Fig. 6A) were nearly identical in structure to proviral inclusions (tubular aggregates) previously shown for paramyxoviruses (Koestner and Long, 1970; Seto et al., 1980). Although more mature filoviral and paramyxoviral inclusions were more easily distinguished, the similar ultrastructure of early inclusions supports the close phylogenetic relationship proposed between filoviruses and paramyxoviruses on the basis of genomic organization and replication strategy. In further support of these familial relationships, Sanchez et al. (1992, 1993) recently demonstrated significant regional nucleoprotein amino acid and genomic sequence homology between MBG and EBO-Z, and paramyxoviruses, and to a lesser extent rhabdoviruses. In contrast with the morphogenic variations previously shown among rhabdoviral serotypes (Matsumoto and Kawai, 1969), our studies did not detect any morphological variations related to susceptible host cells. Structures associated with filoviral and rhabdoviral morphogenesis were clearly distinct.

By employing electron microscopy, we gained further insight into the structure and morphogenesis of filoviruses. The close association of filoviral particles with coated pits along the plasma membranes of challenged cells may demonstrate one potential mechanism for filoviral entry into host cells. Filovirions may have surface ligands and enter the cells by endocytosis. In support, recent studies in other laboratories employed lysosomotropic agents to suggest that MBG penetrates cells by receptor endocytosis (Mariyankova et al., 1993). The first ultrastructural indica-

tion of filoviral infection was the focal accumulation of amorphous material that gradually increased in electron density and progressively occupied larger areas of cytoplasm. As these inclusions of filoviral material developed, they appeared to migrate from the inner regions of the host cell toward the plasma membrane. EBO-S, EBO-Z, and EBO-R nucleocapsids were seen within intermediate inclusions, but MBG nucleocapsids appeared to form directly from inclusion material just before budding. MBG, EBO-S, EBO-Z, and EBO-R nucleocapsids congregated beneath the plasma membrane and acquired viral envelopes as the preformed nucleocapsids budded through the host cell membrane.

IEM showed that all morphologically identifiable filoviral inclusions likely contain both VP40 and NP proteins. The close association of these proteins may be attributed to a net positive charge of the matrix protein (VP40), enabling it to react electrostatically with the negatively charged nucleoprotein (NP) during virus maturation, as noted previously (Elliott et al., 1993). The apparent failure of an anti-EBO-Z GP monoclonal to react with homologous inclusions, concomitant with some gold-sphere labeling of proliferated membranes of EBO-Z-infected cells, supports the belief that surface spikes are acquired as or after preformed nucleocapsids pass through host cell membrane (Murphy et al., 1978). As additional monoclonal antibodies of known specificity are generated and proven, they may be employed in IEM assays to further define the structure and morphogenesis of these emerging pathogens. Future ultrastructural studies should assist in elucidating the replication cycle for filoviruses in susceptible cells. This information may then lend insight into strategic targets for effective intervention using antiviral compounds to combat filoviral infections.

Acknowledgments

We thank Joan Geisbert for preparing the filoviral isolates; Denise Braun and Kathy Keuhl for general EM assistance; and Kelly Davis, Dave Fritz, and Peter Vogel for their critiques of the manuscript. We are grateful to Anthony Sanchez for providing the schematic drawing employed in Fig. 8B.

References

Baskerville, A., Fisher-Hoch, S.P., Nield, G.H. and Dowsett, A.B. (1985) Ultrastructural pathology of experimental Ebola haemorrhagic fever virus infection. J. Pathol. 147, 199–209.

Bowen, E.T.W., Simpson, D.I.H., Bright, W.F., Zlotnik, I. and Howard, D.M.R. (1969) Vervet monkey disease: studies on some physical and chemical properties of the causative agent. Br. J. Exp. Pathol. 50, 400–407.

Bowen, E.T.W., Platt, G.S., Lloyd, G., Raymond, R.T. and Simpson, D.I.H. (1980) A comparative study of strains of Ebola virus isolated from southern Sudan and northern Zaire in 1976. J. Med. Virol. 6, 129–138.

Buchmeier, M.J., DeFries, R.U., McCormick, J.B. and Kiley, M.P. (1983) Comparative analysis of the structural polypeptides of Ebola virus from Sudan and Zaire. J. Infect. Dis. 147, 276–281.

Centers for Disease Control and National Institutes of Health (1984) Biosafety in Microbiological and Biomedical Laboratories: HHS Publication No. (CDC) 86-8395. U.S. Dept. of Health and Human Services, Washington, DC.

Centers for Disease Control (1990) Update: Filovirus infection among persons with occupational exposure to nonhuman primates. M.M.W.R. 39, 266–267.

Ellis, D.S., Bowen, E.T.W., Simpson, D.I.H. and Stamford, S. (1978a) Ebola virus: a comparison, at ultrastructural level, of the behaviour of the Sudan and Zaire strains in monkeys. Br. J. Exp. Pathol. 59, 584–593.

Ellis, D.S., Simpson, D.I.H., Francis, D.P., Knobloch, J., Bowen, E.T.W., Lolik, P. and Deng, I.M. (1978b) Ultrastructure of Ebola virus particles in human liver. J. Clin. Pathol. 31, 201–208.

Ellis, D.S., Stamford, S., Lloyd, G., Bowen, E.T.W., Platt, G.S., Way, H. and Simpson, D.I.H. (1979a) Ebola and Marburg viruses: I. Some ultrastructural differences between strains when grown in Vero cells. J. Med. Virol. 4, 201–211.

Ellis, D.S., Stamford, S., Tovey, D.G., Lloyd, G., Bowen, E.T.W., Platt, G.S., Way, H. and Simpson, D.I.H. (1979b) Ebola and Marburg viruses: II. Their development within Vero cells and the extra-cellular formation of branched and torus forms. J. Med. Virol. 4, 213–225.

Elliott, L.H., Sanchez, A., Holloway, B.P., Kiley, M.P. and McCormick, J.B. (1993) Ebola protein analysis for the determination of genetic organization. Arch. Virol. 133, 423–436.

Feldmann, H., Klenk, H.-D. and Sanchez, A. (1993) Molecular biology and evolution of filoviruses. Arch. Virol. (Suppl.) 7, 81–100.

Geisbert, T.W. and Jahrling, P.B. (1990) Use of immunoelectron microscopy to show Ebola virus during the 1989 United States epizootic. J. Clin. Pathol. 43, 813–816.

Geisbert, T.W., Rhoderick, J.B. and Jahrling, P.B. (1991) Rapid identification of Ebola virus and related filoviruses in fluid specimens using indirect immunoelectron microscopy. J. Clin. Pathol. 44, 521–522.

Geisbert, T.W., Jahrling, P.B., Hanes, M.A. and Zack, P.M. (1992a) Association of Ebola related Reston virus particles and antigen with tissue lesions of monkeys imported to the United States. J. Comp. Pathol. 106, 137–152.

Geisbert, T.W., Jahrling, P.B. and Jaax, N.K. (1992b) Electron and immunoelectron microscopy of experimental Reston virus infection in monkeys. Proc. 50th Ann. EMSA. 1, 682–683.

Geyer, H., Will, C., Feldmann, H., Klenk, H.-D. and Geyer, R. (1992) Carbohydrate structure of Marburg virus glycoprotein. Glycobiology 2, 299–312.

International Committee on Taxonomy of Viruses (1995) Filoviridae. In: F.A. Murphy, C.M. Fauquet, D.H.L. Bishop, S.A. Ghabrial, A.W. Jarvis, G.P. Martelli, M.A. Mayo and M.D. Summers (Eds.), Virus Taxonomy, Classification and Nomenclature of Viruses, Sixth Report of the International Committee on Taxonomy of Viruses, Archives of Virology Supplement 10, pp. 289–292. Springer-Verlag, Vienna.

Jahrling, P.B., Hesse, R.A., Eddy, G.A., Johnson, K.M., Callis, R.T. and Stephen, E.L. (1980) Lassa virus infection of rhesus monkeys: pathogenesis and treatment with ribavirin. J. Infect. Dis. 141, 580–589.

Jahrling, P.B., Geisbert, T.W., Dalgard, D.W., Johnson, E.D., Ksiazek, T.G., Hall, W.C. and Peters, C.J. (1990) Preliminary report: isolation of Ebola virus from monkeys imported to USA. Lancet 335, 502–505.

Kiley, M.P., Bowen, E.T.W., Eddy, G.A., Isaacson, M., Johnson, K.M., McCormick, J.B., Murphy, F.A., Pattyn, S.R., Peters, D., Prozesky, O.W., Regnery, R.L., Simpson, D.I.H., Slenczka, W., Sureau, P., van der Groen, G., Webb, P.A. and Wulff, H. (1982) Filoviridae: a taxonomic home for Marburg and Ebola viruses? Intervirology 18, 24–32.

Kiley, M.P., Cox, N.J., Elliott, L.H., Sanchez, A., DeFries, R., Buchmeier, M.J., Richman, D.D. and McCormick, J.B. (1988) Physiochemical properties of Marburg virus: evidence for three distinct virus strains and their relationship to Ebola virus. J. Gen. Virol. 69, 1957–1967.

Kissling, R.E., Robinson, R.Q., Murphy, F.A. and Whitfield, S.G. (1968) Agent of disease contracted from green monkeys. Science 160, 888.

Kissling, R.E., Murphy, F.A. and Henderson, B.E. (1970) Marburg virus. Ann. NY. Acad. Sci. 174, 932–945.

Koestner, A. and Long, J.F. (1970) Ultrastructure of canine distemper virus in explant tissue cultures of canine cerebellum. Lab. Invest. 23, 196–201.

Mariyankova, R.F., Giushakova, S.E., Pyzhik, E.V. and Lukashevich, I.S. (1993) Marburg virus penetration into eukaryotic cells. Vopr. Virusol. 2, 74–76.

Matsumoto, S. and Kawai, A. (1969) Comparative study on development of rabies virus in different host cells. Virology 39, 449–459.

McClave, J.T. and Dietrich, F.H., II (1988) Bonferroni test. In: J.T. McClave and F.H. Dietrich II (Eds.), Statistics. Dellen Publishing Co., San Francisco, CA, p. 495.

McCormick, J.B., Bauer, S.P., Elliott, L.H., Webb, P.A. and Johnson, K.M. (1983) Biological differences between strains of Ebola virus from Zaire and Sudan. J. Infect. Dis. 147, 264–267.

Murphy, F.A., Simpson, D.I.H., Whitfield, S.G., Zlotnik, I. and Carter, G.B. (1971) Marburg virus infection in Monkeys. Lab. Invest. 24, 279–291.

Murphy, F.A., van der Groen, G., Whitfield, S.G. and Lange, J.V. (1978) Ebola and Marburg virus morphology and taxonomy. In: S.R. Pattyn (Ed.), Ebola Virus Haemorrhagic Fever. Elsevier/North-Holland Biomedical Press, Amsterdam, pp. 61–82.

Murphy, F.A., Kiley, M.P. and Fisher-Hoch, S.P. (1990) Filoviridae. Marburg and Ebola viruses. In: B.N. Fields and D.M. Knipe (Eds.), Virology. Raven Press Ltd., New York, pp. 933–942.

Pringle, C.R. (1991) The order Mononegavirales. Arch. Virol. 117, 137–140.

Sanchez, A., Kiley, M.P., Klenk, H.-D. and Feldmann, H. (1992) Sequence analysis of Marburg virus nucleoprotein gene: comparison to Ebola virus and other non-segmented negative-strand RNA viruses. J. Gen. Virol. 73, 347–357.

Sanchez, A., Kiley, M.P., Holloway, B.P. and Auperin, D.D. (1993) Sequence analysis of the Ebola virus genome: organization, genetic elements and comparison with the genome of Marburg virus. Virus Res. 29, 215–240.

Schnittler, H.-J., Mahner, F., Drenckhanh, D., Klenk, H.-D. and Feldmann, H. (1993) Replication of Marburg virus in human endothelial cells. J. Clin. Invest. 91, 1301–1309.

Seto, J.T., Wahn, K. and Becht, H. (1980) Electron microscope study of cultured cells of the chorioallantoic membrane infected with representative paramyxoviruses. Arch. Virol. 65, 247–255.

Siegert, R., Shu, H.-L., Slenczka, W., Peters, D. and Müller, G. (1967) Zur Atiologie einer unbekannten, von Affen ausgegangenen menschlichen Infektionskrankheit. Dtsch. Med. Wochenschr. 92, 2341.